Detailed features of the surface electronic states of K/Cu(111) by density functional theory

S. Achilli,[1] M. I. Trioni,[2] and G. P. Brivio[1]
[1]*CNISM, ETSF, Dipartimento di Scienza dei Materiali, Università di Milano-Bicocca, Via Cozzi 53, 20125 Milano, Italy*
[2]*CNISM and CNR-INFM, UdR Milano Bicocca, Via Cozzi 53, 20125 Milano, Italy*
(Received 26 October 2009; revised manuscript received 1 April 2010; published 29 April 2010)

The surface states generated by the adsorption of a full monolayer of K on Cu(111) are obtained by the embedding method within density functional theory. Their energy dependence is accounted for as function of the surface parallel wave vector and is connected to the spatial distribution of the electronic charge computed at special points in the two-dimensional Brillouin zone. Thanks to the description of a truly semi-infinite substrate within the adopted framework, the elastic linewidth of the surface states is determined with great accuracy and is shown to reflect the different degrees of hybridization of such states with the surface projected bulk bands.

DOI: 10.1103/PhysRevB.81.165444 PACS number(s): 73.20.At, 73.21.Fg, 73.61.At

I. INTRODUCTION

Several very interesting phenomena occur when alkali atoms adsorb on a metal surface. A well-known effect is a drastic change in the work function. In fact at low alkali coverage such a function is strongly reduced, it increases again when more than half monolayer (ML) is formed, and eventually saturates at 1 ML, still remaining few electron volt below the clean metal one. This process was essentially explained in the pioneering work of Langmuir[1] first as the effect of the complete ionization of the alkali adsorbates at lower coverages, then of their consequent depolarization at higher ones. This model was later supported by the quantum-mechanical treatment of Gurney[2] and by several systematic studies based on density functional theory (DFT) on jellium[3] and on an atomistic solid[4,5] (for a review see Ref. 6), which show the partial ionic character of the alkali atom-surface bond. Nevertheless the nature of the alkali adsorbate-substrate bond was long debated. Alternative models suggested that the adatom valence charge cloud is strongly localized in the region between the adatom and the surface,[7] and from DFT calculations on jellium that the adatom-surface interaction may form a covalent bond.[8] Owing to the relative simplicity of the electronic structure, surface geometry, and adatom-adatom interaction, the alkali atoms adsorbed on metals are still subject of numerous investigations as bench mark systems for more complex ones. The investigated properties include adsorbate-induced surface states,[9–11] surface diffusion,[12,13] lateral interactions,[14] and lifetimes of excited states.[15]

Alkali atoms on noble metals have been recently subject of several experimental and theoretical investigations focused on their surface states.[15] According to the hybridization between substrate and alkali states the surface electronic structure of the clean metal is significantly modified in different ways. New surface resonant features already appear upon deposition of a single atom. They evolve during the growth leading to surface states with an energy tunable with coverage. At completion of 1 ML the following main surface states have been observed: the modified Shockley state of the clean surface; the quantum well state (QWS) showing a discrete energy in the surface perpendicular direction, and a two-dimensional electron-gas parabolic dispersion as a function of the surface wave vector; long living image states (IS), which are usually probed by two-photon photoemission spectroscopy[16] and scanning tunneling spectroscopy;[17] and the gap excited state.

In quite a few cases these alkali-induced features have attracted large interest due to their extremely long lifetime. In particular, the quantum well state and its precursor at very low coverage display a very small linewidth, on the order of tens of millielectron volt.[18,19] This property opens up the measurement of the surface dynamics of electrons. First we recall that the interaction between an excited surface state induced by the adatom and a resonant substrate continuum determines a decay of the former by a resonant charge-transfer process to the metal. Hence the time dependent survival amplitude worked out by projecting the initial surface state onto its evolving wave function displays a decay rate which generates the so-called elastic lifetime. Second that other effects contribute to the measured decay rate. Three more important ones are the inelastic electron-electron and electron-phonon interactions and the effect due to impurity scattering.[20]

Alkali adsorption on Cu(111) is particularly interesting since the surface projected band of this metal displays a wide energy gap at the $\bar{\Gamma}$ point in the surface Brillouin zone (SBZ). For these systems surface states lying in such a gap only show a very small elastic contribution to the lifetime due to bulk band folding. If such an effect may be neglected the measured linewidths could provide results only on the inelastic electron-electron and electron-phonon lifetimes. Larger hybridization with the substrate states characterizes alkali-induced electronic features in other dispersion regions of the SBZ so that their linewidths are mainly determined by the elastic term.

The calculation of the various contributions to the lifetime of adatom-induced surface states has been the subject of many works.[17,21–23] We have tackled it by the Green's function embedding approach[24,25] extended to realistic surfaces,[26] within the DFT framework. This method allows for considering a truly semi-infinite substrate. So it permits to distinguish between discrete and resonant states providing also an accurate estimate of the contribution of the elastic linewidth

of the latter ones. In recent years we have investigated the surface electronic properties of Na/Cu(111) (Ref. 10) and Cs/Cu(111) (Ref. 11) by such an approach. The investigation of the electronic states of another alkali adatom, namely, the system K/Cu(111) is also interesting for the above-mentioned reasons. Moreover results from photoemission spectroscopy have been recently published.[27] But we do not just wish to present a numerical study to be compared with experiments.[27,28] In fact our work also includes detailed calculations of the band dispersion, the charge contours, and a very accurate estimate of the linewidths of the surface states as a function of the surface parallel wave vector.

In the next section the structural properties of K/Cu(111) together with an outline of the embedding method will be presented. Section III deals with the numerical results and their discussion while Sec. IV is devoted to conclusions.

II. DESCRIPTION OF K/Cu(111)

A. Structural configuration

The adsorption of alkali atoms on Cu(111) has been the subject of several studies addressing the evolution of the surface structural properties on varying coverages.[6,29–32] In fact, due to the low corrugation of the Cu(111) surface, the adatoms are almost free to rearrange themselves, leading to a series of submonolayer surface reconstructions superimposed to the underlying Cu(111) lattice structure. For K/Cu(111) at low coverages, which displays hexagonal structure with the same orientation as that of the substrate, incommensurate surface reconstructions have also been observed. Since we are interested in the properties of a single atomic layer, we recall that in alkali overlayers the definition of 1 ML is often expressed in term of the nominal coverage ϑ (defined as the ratio of the number of adatoms to the number of substrate atoms per unit area) characterizing the ordered reconstruction that gives the maximum photoemission intensity of the K-induced state near the Fermi level. Fischer *et al.*[28,33] showed that the completion of the K first overlayer occurs in correspondence of an ordered (2×2) low-energy electron diffraction (LEED) pattern, near the saturation coverage of the work function.

A detailed analysis of LEED data shows in addition a linear relationship between the inverse square of K nearest-neighbor spacing and the amount of K adatoms, which reflects the formation of a hexagonal overlayer. Such a relation is valid up to a nominal coverage of about $\vartheta=0.3$ (allowing for some experimental uncertainty), which is in agreement with an exact $K(2\times2)$ phase ($\vartheta=0.25$) at completion of the first layer. Further adsorption of K, determining saturation at about $\vartheta=0.4$, is expected to lead to out-of-plane reconstructions.[29]

Since our theoretical results calculated for the $K(2\times2)$ phase will be also compared with the experimental ones reported in Ref. 27, it is important to critically examine the definition of coverage used in that paper. In fact such authors assign a coverage of 0.75 ML, considerably lower than 1 ML, to the $K(2\times2)$ commensurate reconstruction at variance with the previous definition. This discrepancy may be explained by assuming a nominal coverage of $\vartheta=0.4$ at the completion of the first adatom overlayer which would define 1 ML. Restoring the more appropriate value close to $\vartheta=0.3$, as discussed above, the first $K(2\times2)$ reconstruction is compatible with 1.0 ML coverage, due to the uncertainties reported in the experimental works.[6,28,33] For these reasons we have compared our electronic properties of the perfect (2×2) reconstruction with those of the 0.9–1 ML reported in Ref. 27. The optimal agreement between several of such experimental results and those calculated in this paper *a posteriori* confirms our structural working assumption.

The K atoms adsorb in atop position, as confirmed both by surface-extended x-ray-absorption fine structure (SEXAFS) experiments[34] and theoretical simulations.[35–37] We use the experimental K-Cu distance of 3.05 Å as determined by SEXAFS experiments. The lattice parameter of clean Cu (3.61 Å) and the surface relaxation are the measured ones. We wish to remark that we could carry out a calculation of such parameters within the same DFT framework of the computed surface states. However, aim of this paper is the evaluation of the electronic spectral properties of a realistic potassium overlayer on Cu(111). To this purpose the best input atomic configuration is the experimental one, as already discussed.[10]

B. Theoretical model of the electronic surface states

In order to compute the electronic states, we make use of the Green's function embedding approach.[38] This method has already been discussed in detail elsewhere,[13,25,26] so we only outline its main points here. First all the space is divided into two regions: in the former, say II, of higher symmetry the one-particle Green's function, $G_0(\mathbf{r},\mathbf{r}',E)$ is known with the desired accuracy; in the latter region I, of lower symmetry, the Green's function, $G(\mathbf{r},\mathbf{r}',E)$, is solution of the following Schrödinger-type equation (atomic units are used hereafter unless differently specified):

$$\left[-\frac{1}{2}\nabla^2+v_{eff}(\mathbf{r})-E\right]G(\mathbf{r},\mathbf{r}',E)+\delta(\mathbf{r}-\mathbf{r}_s)\times\left[\frac{1}{2}\frac{\partial G(\mathbf{r}_s,\mathbf{r}',E)}{\partial n_s}+\int_S d\mathbf{r}_s''G_0^{-1}(\mathbf{r}_s,\mathbf{r}_s'',E)G(\mathbf{r}_s'',\mathbf{r}',E)\right]=\delta(\mathbf{r}-\mathbf{r}')\mathbf{r},\quad \mathbf{r}'\in \mathrm{I}. \tag{1}$$

Note that the integral is performed only over the surface S, of normal unit vector n_s, separating the two regions, while the function $G_0^{-1}(\mathbf{r}_s,\mathbf{r}_s'',E)$, the surface spatial inverse of $G_0(\mathbf{r},\mathbf{r}',E)$ satisfying the vanishing von Neumann boundary condition on S, is a nonlocal energy dependent potential which ensures that the solution inside region I correctly matches that outside it. The local potential $v_{eff}(\mathbf{r})$ is the effective potential of the Kohn-Sham approach of DFT calculated within the generalized gradient approximation (GGA).[39] We use a linearized augmented plane-wave full-potential method.

We shall focus on the computation of the imaginary diagonal part of the Green's function, say $(-1/\pi)\Im m G_{\mathbf{k}_\parallel}(\mathbf{r},\mathbf{r},E)$. In fact from such a function we can obtain the charge density and, by integrating it in a suitable region of space, the $\mathbf{k}_\parallel$

resolved density of states (DOS), $\sigma(\mathbf{k}_\parallel, E)$. Since we are interested in the electronic properties of the adatom-induced surface states we work out $\sigma(\mathbf{k}_\parallel, E)$ in the muffin tin (MT) of the K adatom. By the embedding approach surface states which lie in a surface projected band gap will be exactly described, at any $\mathbf{k}_\parallel$, by discrete ones in the normal energy component while resonant ones will naturally display a linewidth without any *ad hoc* broadening as in supercell method. Such a linewidth is usually called the elastic one.

It is well known that DFT in its GGA implementation cannot account correctly for the image potential. A rigorous method beyond the usual DFT capable to get the image potential is the GW approximation[40,41] which however requires a huge increase in computational time. A simpler alternative is to consider the following phenomenological approach,[42,43] which takes into account an embedding potential on the surface vacuum side deduced by an effective potential v_{eff} with the asymptotic correct decay. After the self-consistent procedure solving Eq. (1) is completed, the effective potential v_{eff} is gradually mixed with the model image potential $-1/4|z-z_{im}|$. A final iteration in Eq. (1) with such potential is enough to get the correct energy of the image states. In particular, such a modified effective potential v_{eff}^{im} is defined as

$$v_{eff}^{im}(z) = [1 - I_z(a,b)]v_{eff}(z) + I_z(a,b)\left[-\frac{1}{4|z-z_{im}|}\right]. \quad (2)$$

In Eq. (2) $I_z(a,b)$ is an incomplete beta function. Note that the results are very weakly dependent on the choice of the parameters a and b. The coordinate z_{im} is the image plane position; its determination is discussed in Ref. 10.

The calculation was performed within an embedded region that extends in the z direction for 13.75 Å and includes two Cu layers, the adatom overlayer and a portion of vacuum 7.5 Å wide. The Green's function was expanded using 120 Ry as a cutoff for the kinetic part, the MT radii are 1.21 Å and 1.72 Å for Cu and K, respectively. We used $l_{\max}=9$ for the spherical expansion inside the MT. The SBZ is sampled by a 9×9 mesh while the image plane position is taken at $z_{im}=1.95$ Å from the K nuclei.

III. RESULTS

In this section we present the calculated electronic properties of the system (2×2) K/Cu(111). We note first that the agreement between the computed and experimental work functions, which amount to $\Phi_{\text{th}}=4.89$ eV and $\Phi_{\text{exp}}=4.93$ eV, respectively, is very good for the clean metal surface. For the alkali adsorbate system there is a difference of about 10% as large as that for (2×2) Na/Cu(111),[10] namely, $\Phi_{\text{th}}=2.07$ eV and $\Phi_{\text{exp}}=2.27$ eV. This difference may be ascribed to differences between the perfectly ordered (2×2) reconstruction of the calculation and the real surface structure which may contain impurities and defects.

In order to characterize the alkali-induced electronic states we discuss now the properties of the $\mathbf{k}_\parallel$ resolved DOS. We remark that the DOS at $\bar{\Gamma}$ point, reported in Fig. 1, is already able to show the main surface electronic states of this system. By setting the reference energy at the Fermi level E_F,

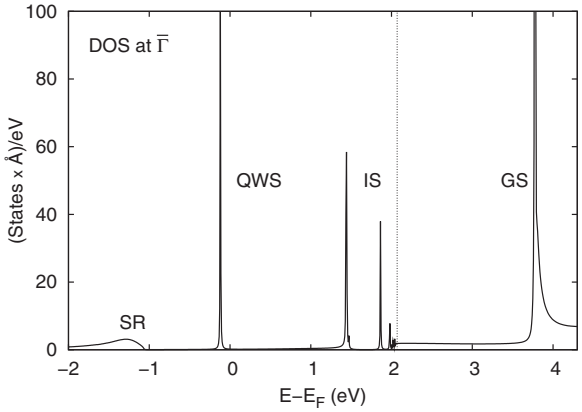

FIG. 1. DOS at the $\bar{\Gamma}$ point evaluated in the alkali atomic MT of (2×2) K/Cu(111). The dotted vertical line represents the vacuum level.

we observe first a weak broad feature between −2 and −1 eV due to the so-called surface resonance (SR). It derives from the Shockley state of the clean metal surface whose energy is shifted down by alkali adsorption.[15,27] Next, just below E_F, note the much sharper peak of the QWS, which arises mainly from the K 4s resonance. Such a state is peaked above E_F for an isolated adatom but its energy lowers by increasing the adsorbate coverage as a direct consequence of the dipole interaction between adsorbed alkalis which generates a local electric field on the neighboring atomic sites. This effect somewhat saturates at about 0.7 ML where the overlap of the adsorbate orbitals leading to the metallization is considerable.[44] The IS series follows within the energy range 1.37–2.07 eV and, after the weak vacuum states contribution, finally the so-called electron gap state (GS) appears at energies about 1.8 eV above the vacuum level. Such a state, already discussed for Cs/Cu(111),[11] is due to the folding of the SR. At $\bar{\Gamma}$ point all states display an elastic width but the image ones and the GS, which lie in the gap of the surface projected and folded bulk band. They are assigned a small nonphysical width just to plot them in Figs. 1 and 3. In particular, the GS merges into a higher energy surface projected band.

Further characterization of the electronic states can be obtained by their spatial charge-density distribution and by their surface planar average (SPA). Those quantities are plotted at $\bar{\Gamma}$ in Fig. 2 for all the surface states, except the image ones that are known to live very far from the surface. The charge distribution of the SR (upper left panel) shows states of p character on the Cu atoms. Around K such contours are instead spherical and of lower intensity reflecting s like behavior and charge depletion, in agreement with the results for the unsupported K monolayer.[45] The SPA for this state is mainly localized in the surface region. The charge contours of the QWS (upper middle panel) are at variance with those of the previous case. Charge in the region between the adatom and the metal layer is scarce and is spilled out from the K atom to vacuum signaling an outward spatial distribution of the QWS as confirmed by its SPA. The shape of the

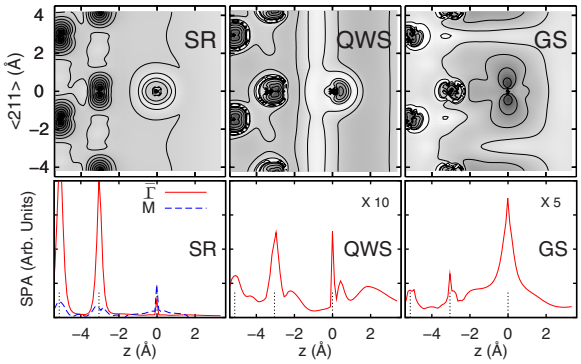

FIG. 2. (Color online) (2×2) K/Cu(111). Upper three panels: surface charge-density contours at $\bar{\Gamma}$ of GS, QWS, and SR, from right to left. Darker (lighter) regions correspond to larger (smaller) electron density. Lower three panels: SPA of the charge density at $\bar{\Gamma}$ for the same states. SR SPA at $\bar{M}$ (dashed line). Vertical dotted lines denote Cu and K nuclei.

charge-density contours around K of the GS (upper right panel) may be interpreted as due to a *p-d* admixture of states.[45] The SPA of this state is peaked at the atom position in agreement with the result for Cs/Cu(111).[11]

In Fig. 3 we display the function $\sigma(\mathbf{k}_{\parallel},E)$ along the high-symmetry paths in the SBZ in a three-dimensional plot. We describe now the spectrum from $\bar{\Gamma}$ to $\bar{M}$ in more detail. At about 1 eV below E_F the rather broad and weak feature of the SR increases in energy until $\bar{M}$ point where it crosses the lower branch of the GS. We verified that the SR gets a stronger overlayer character near the zone boundaries, as already reported for K (Ref. 27) and Cs (Ref. 11) on Cu(111), by computing its SPA at the $\bar{M}$ point. Note that this function is plotted as a dashed line in the left lower panel of Fig. 2. The QWS sharp peak at $\bar{\Gamma}$ weakens and merges into the surface projected bulk band edge near $\bar{M}$. The series of IS's are neatly observable along most of the dispersion curve. Finally the GS separates in two branches that interact differently with the image states.

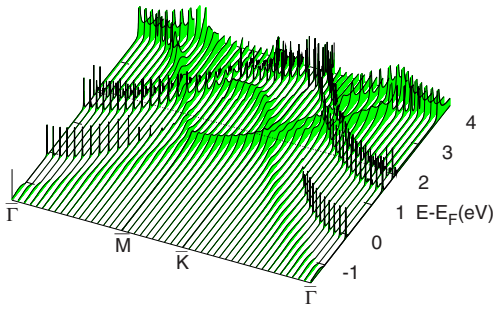

FIG. 3. (Color online) Surface band structure of (2×2) K/Cu(111) along the high-symmetry paths.

For comparison with previous experimental results along the $\bar{\Gamma}\bar{M}$ direction we have performed a parabolic fit of the calculated dispersion of the QWS, SR, and IS's. Their binding energy at $\bar{\Gamma}$, effective mass, Fermi wave vector k_F, and the elastic linewidth Γ_{el} at $\bar{\Gamma}$ are reported in Table I. The agreement with the experimental data is overall good. The largest disagreement with experiments is displayed by the SR binding energy and is related to the well-known problem of estimating correctly bulk valence-band edges in DFT. In fact this resonance state lies at the upper edge of the *sp* bulk band which hybridizes with and consequently is forced to follow its energy behavior. Since we verified that the upper edge of the *sp* band of copper calculated by DFT lies 0.2 eV below the experimental value, the SR shifts downward of about the same amount.

Comparing the theoretical results for K/Cu(111) with the previous studies of Cs and Na at the saturation coverage on the same surface, we observe that the binding energy of the QWS at $\bar{\Gamma}$ point decreases by increasing the adatom atomic number. Note that the Na- and K-induced QWS are occupied while that of Cs lies above the Fermi level.[13] The different position within the energy gap determines the effective mass of such states, which tends to the free particle one going from Na to Cs, as expected.

Along the $\bar{\Gamma}\bar{M}\bar{K}\bar{\Gamma}$ path the surface states mutually cross and broadening processes due to the hybridization with the

TABLE I. Key features of the surface states of (2×2) K/Cu(111) (in brackets the experimental values).

State	Energy[a,b] (eV)	k_F (Å^{-1})	Effective mass (m_e)	Elastic width[b] (meV)
SR	−1.28(∼−1.03)[c]	0.43 (∼0.36)[c]	0.53 (0.55)[c]	∼250
QWS	−0.118(−0.100)[c]	0.148 (∼0.15)[c]	0.707 (0.81)[c]	∼2.8
GS	3.8			∼0
IS $n=1$	−0.626(−0.64 ± 0.03)[d]		0.92	0
IS $n=2$	−0.208(−0.19)[d]		0.95	0
IS $n=3$	−0.090(−0.05)[d]		0.95	0

[a]For the image states the reference energy is the vacuum level.
[b]At $\bar{\Gamma}$.
[c]Reference 27.
[d]Reference 28.

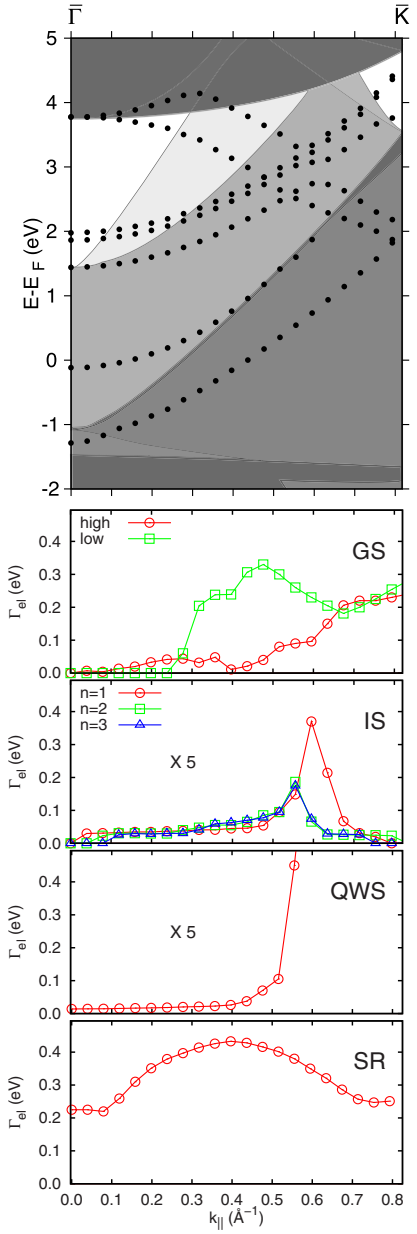

FIG. 4. (Color online) Dispersion (dots) of the surface states on the surface projected bulk band structure of the (2×2) K/Cu(111) reconstruction (top panel). For details see text. Linewidths of the surface states as function of $\mathbf{k}_\parallel$ (four bottom panels).

surface projected bulk bands as function of $\mathbf{k}_\parallel$ determine a complex variations in their linewidth. In order to analyze such features, in the top panel of Fig. 4 we report a different representation of the dispersion along the $\overline{\Gamma K}$ path. In the background observe the surface projected bands of clean Cu(111) and those determined by the folding in the (2×2) reconstruction, which are plotted with different shades of gray. White areas denote the remaining gaps and continuous lines the band edges. The maxima of surface states along the $\overline{\Gamma K}$ path are denoted by dark dots. They have been obtained together with their linewidths by a Lorentzian fit of the corresponding peaks in the $\mathbf{k}_\parallel$ dependent DOS. In the four panels of Fig. 4 beneath, the calculated linewidths of the surface states are plotted as a function of $\mathbf{k}_\parallel$. As expected, the main changes in a surface state occur when it enters into a continuous bulk band or when it crosses other surface states. The former point has different effects if the bulk band belongs to the (1×1) SBZ of the clean substrate or derives from its folding due to the adlayer-induced reconstruction. See, for example, the QWS. Near $\bar{\Gamma}$ it displays a very small linewidth due to the interaction with a folded band. But Γ_{el} abruptly increases when the state enters in the nonfolded projected bulk band around 0.50 Å^{-1}. The same effect occurs for the SR when it merges into a folded band near 0.1 Å^{-1}. A strong increase in the linewidth due to surface state crossing is instead shown by the image states when they intersect the two branches of the GS. Note also that very near $\bar{\Gamma}$ the linewidths of the IS tend to zero since such states lie in a gap of the surface projected bulk and folded bands. It is also interesting to point out the avoided crossing of the higher branch of the GS with the $n=1$ image state at about $\mathbf{k}_\parallel=0.6$ Å^{-1} due to symmetry reasons. The values of the linewidth at $\bar{\Gamma}$ are reported in Table I.

IV. CONCLUSIONS

In this paper we have presented a fairly thorough survey of the surface states of (2×2) K/Cu(111) at 1 ML of coverage computed by the embedding method within the DFT framework. We point out first that such a Green's-function approach is most suitable to reproduce the spectral properties since it assumes a truly semi-infinite solid. The surface-state dispersions along high-symmetry paths and the charge densities have been described in detail. We have been able to disentangle features due to the hybridization of the surface states with the clean metal and with the folded surface projected bands. Energies and effective masses show good agreement with previous experimental works. We have also found many analogies with the surface-state properties of other alkali atoms on Cu(111) systems. Second we have focused on the elastic linewidths of the surface states. Such delicate analysis can be performed by the embedding approach in a very accurate way and points out that these linewidths show a wealth of different shapes and magnitudes by varying the surface parallel wave vector. In conclusion we believe that the theoretical investigation presented in this paper of the surface-state properties, as a function of the parallel wave vector, of (2×2) K/Cu(111), could be a useful tool to elucidate experimental features of excited states also measured in terms of the emission angle.

ACKNOWLEDGMENT

We are grateful to G. Fratesi and H. Ishida for a critical reading of the manuscript.

[1] I. Langmuir and J. B. Taylor, Phys. Rev. **40**, 463 (1932).
[2] R. W. Gurney, Phys. Rev. **47**, 479 (1935).
[3] N. D. Lang and A. R. Williams, Phys. Rev. B **18**, 616 (1978).
[4] M. Scheffler, C. Droste, A. Fleszar, F. Máca, G. Wachutka, and G. Barzel, Physica B **172**, 143 (1991).
[5] J. Bormet, J. Neugebauer, and M. Scheffler, Phys. Rev. B **49**, 17242 (1994).
[6] R. D. Diehl and R. McGrath, Surf. Sci. Rep. **23**, 43 (1996).
[7] G. K. Wertheim, D. M. Riffe, and P. H. Citrin, Phys. Rev. B **49**, 4834 (1994).
[8] H. Ishida, Phys. Rev. B **38**, 8006 (1988).
[9] J. M. Carlsson and B. Hellsing, Phys. Rev. B **61**, 13973 (2000).
[10] G. Butti, S. Caravati, G. P. Brivio, M. I. Trioni, and H. Ishida, Phys. Rev. B **72**, 125402 (2005).
[11] V. Chis, S. Caravati, G. Butti, M. I. Trioni, P. Cabrera-Sanfelix, A. Arnau, and B. Hellsing, Phys. Rev. B **76**, 153404 (2007).
[12] G. Alexandrowicz, A. P. Jardine, H. Hedgeland, W. Allison, and J. Ellis, Phys. Rev. Lett. **97**, 156103 (2006).
[13] G. P. Brivio, G. Butti, S. Caravati, G. Fratesi, and M. I. Trioni, J. Phys.: Condens. Matter **19**, 305005 (2007).
[14] J. Ellis, A. P. Graham, F. Hofmann, and J. P. Toennies, Phys. Rev. B **63**, 195408 (2001).
[15] J. P. Gauyacq, A. G. Borisov, and M. Bauer, Prog. Surf. Sci. **82**, 244 (2007).
[16] M. Weinelt, A. B. Schmidt, M. Pickel, and M. Donath, Prog. Surf. Sci. **82**, 388 (2007).
[17] J. Kröger *et al.*, Prog. Surf. Sci. **82**, 293 (2007).
[18] S. Ogawa, H. Nagano, and H. Petek, Phys. Rev. Lett. **82**, 1931 (1999).
[19] M. Bauer, S. Pawlik, and M. Aeschlimann, Phys. Rev. B **60**, 5016 (1999).
[20] V. M. Silkin, A. Balassis, A. Leonardo, E. V. Chulkov, and P. M. Echenique, Appl. Phys. A: Mater. Sci. Process. **92**, 453 (2008).
[21] C. Corriol, V. M. Silkin, D. Sánchez-Portal, A. Arnau, E. V. Chulkov, P. M. Echenique, T. von Hofe, J. Kliewer, J. Kröger, and R. Berndt, Phys. Rev. Lett. **95**, 176802 (2005).
[22] A. G. Borisov *et al.*, Phys. Rev. Lett. **101**, 266801 (2008).
[23] S. Achilli, G. Butti, M. I. Trioni, and E. V. Chulkov, Phys. Rev. B **80**, 195419 (2009).
[24] J. E. Inglesfield, Surf. Sci. **76**, 355 (1978).
[25] G. P. Brivio and M. I. Trioni, Rev. Mod. Phys. **71**, 231 (1999).
[26] H. Ishida, Phys. Rev. B **63**, 165409 (2001).
[27] F. Schiller, M. Corso, M. Urdanpilleta, T. Ohta, A. Bostwick, J. L. McChesney, E. Rotenberg, and J. E. Ortega, Phys. Rev. B **77**, 153410 (2008).
[28] N. Fischer, S. Schuppler, R. Fischer, Th. Fauster, and W. Steinmann, Phys. Rev. B **47**, 4705 (1993).
[29] W. C. Fan and A. Ignatiev, Phys. Rev. B **37**, 5274 (1988).
[30] D. Tang, D. McIlroy, X. Shi, C. Su, and D. Heskett, Surf. Sci. **255**, L497 (1991).
[31] X. Shi, C. Su, D. Heskett, L. Berman, C. C. Kao, and M. J. Bedzyk, Phys. Rev. B **49**, 14638 (1994).
[32] W. C. Fan and A. Ignatiev, J. Vac. Sci. Technol. A **6**, 735 (1988).
[33] N. Fischer, S. Schuppler, Th. Fauster, and W. Steinmann, Surf. Sci. **314**, 89 (1994).
[34] D. L. Adler *et al.*, Phys. Rev. B **48**, 17445 (1993).
[35] L. Padilla-Campos, A. Toro-Labbé, and J. Maruani, Surf. Sci. **385**, 24 (1997).
[36] L. Padilla-Campos and A. Toro-Labbé, J. Chem. Phys. **108**, 6458 (1998).
[37] K. Doll, Eur. Phys. J. B **22**, 389 (2001).
[38] J. E. Inglesfield, J. Phys. C **14**, 3795 (1981).
[39] J. P. Perdew, K. Burke, and M. Ernzerhof, Phys. Rev. Lett. **77**, 3865 (1996).
[40] A. G. Eguiluz, M. Heinrichsmeier, A. Fleszar, and W. Hanke, Phys. Rev. Lett. **68**, 1359 (1992).
[41] G. Fratesi, G. P. Brivio, P. Rinke, and R. W. Godby, Phys. Rev. B **68**, 195404 (2003).
[42] M. Nekovee and J. E. Inglesfield, Europhys. Lett. **19**, 535 (1992).
[43] M. Nekovee and J. E. Inglesfield, Prog. Surf. Sci. **50**, 149 (1995).
[44] H. Ishida, Phys. Rev. B **40**, 1341 (1989).
[45] E. Wimmer, J. Phys. F: Met. Phys. **13**, 2313 (1983).